Weather and Climate Extremes xxx (xxxx) xxxx

Contents lists available at ScienceDirect

Weather and Climate Extremes

journal homepage: www.elsevier.com/locate/wace

Watershed-scale retrospective drought analysis and seasonal forecasting using multi-layer, high-resolution simulated soil moisture for Southeastern U.S

Vinit Sehgal[a,b], Venkataramana Sridhar[a,*]

[a] Department of Biological Systems Engineering, Virginia Polytechnic Institute and State University, Virginia, 24061, USA
[b] Water Management and Hydrological Science, Texas A&M University, Texas, USA

ARTICLE INFO

Keywords:
Soil moisture
SWAT
CFSv2
Drought
Southeastern US
Multi-layer

ABSTRACT

Drought assessment at local scales needs a reliable framework capturing both local landscape processes and the watershed-scale hydrological responses. Any such tool, implementable in a near real-time, semi-automated framework, is largely unavailable for the South Atlantic-Gulf (SAG) region in the Southeastern US (SEUS). In this study, we evaluate a drought monitoring and forecasting approach using multi-layer, high resolution, simulated soil moisture for 50 watersheds in the SEUS. Soil and Water Assessment Tool (SWAT) is integrated with meteorological drivers (precipitation and temperature) from Climate Forecast System Reanalysis data (CFSR) for retrospective simulations (January 1982–December 2013), and Climate forecast system model version-2 (CFSv2) models to obtain the near real-time estimates (January 2014 through mid-March 2017) and 9-month lead forecasts (mid-March through December 2017) of the hydrologic variables at 12-digit Hydrologic Unit Code (HUC-12) resolution. Drought assessment is carried out by combining the drought severity estimates of the weekly percentiles of the surface and total column (TC) soil moisture, aggregated to 4-week and 8-week respectively, following a different severity classification scheme for each layer. Several drought indices and observed drought maps from the U.S. Drought Monitor (USDM) are used to compare the agreement (or disagreement) of the proposed approach with the observed drought conditions in the region. The results show promising application of the proposed approach for near real-time estimation as the drought estimates show high (~80–90%) Index of Agreement (IOA) with the Palmer Drought Severity Index (PDSI) for all drought categories (mild-exceptional). The retrospective assessment shows that TC soil moisture percentiles have high correlation (> 0.7) with long-term drought indices. The surface soil moisture percentiles show high correlation (~0.6) with Palmer Z Index (ZNDX) and 1-month Standardized Precipitation Index (SPI-1), while longer aggregations increase the association with the long-term drought indices. While the SWAT-CFSv2 based drought estimation is useful in near real-time mode, higher disagreement between the forecasted drought maps and the observed drought severity from the USDM is noted for a forecast window of greater than ~ 4–6 weeks.

1. Introduction

Droughts produce a complex set of transboundary impacts that influence all components of the hydrologic budget, namely, the supply, storage, and flux (precipitation, soil moisture, snowmelt, ground and surface water, and evapotranspiration) and have costly socio-economic consequences. These calamities are the result of climate variations that infrequently occur in vast geographic regions (Kang and Sridhar, 2017; Thilakarathne and Sridhar, 2017; Zou et al., 2017). The Southeastern U.S. (SEUS) has experienced widespread droughts three times within past 15 years (Sehgal and Sridhar, 2018). These droughts have not only caused enormous strain on the agriculture and farms activities in the region but have also heightened instances of wildfires in the region, especially in the Appalachian region (Scasta et al., 2016). Increasing drought vulnerability of the SEUS region is linked to continued industrial and population growth, leading to increased industrial, agricultural and metropolitan water demand (Manuel, 2008; Pederson et al., 2012; Seager et al., 2009). It is important to note that the SEUS is expected to have the largest absolute increase in population compared to any other region in the U.S. by 2030 (Nagy et al., 2011; U.S. Census Bureau, 2005). Water is a limited resource, and the threat of water-related conflict in the region has the potential to grow more intense in

* Corresponding author.
E-mail address: vsri@vt.edu (V. Sridhar).

https://doi.org/10.1016/j.wace.2018.100191
Received 10 April 2018; Received in revised form 18 July 2018; Accepted 12 December 2018

the coming decades (Sehgal and Sridhar, 2018). Hence, utilizing information from seasonal climate forecast and long-term climate prediction for effective drought monitoring and forecasting has proven to be of great interest to water planners and decision makers to improve preparedness towards, and mitigation of impacts due to climatic extremes (Hansen, 2005; Shafiee-Jood et al., 2014).

Soil moisture has a significant impact on important meteorological and hydrological processes like *(i)* the development of mesoscale circulations between land surface patches with differing soil moisture conditions *(ii)* the development of deep convection *(iii)* the growth and sustainment of large-scale interannual variations such as droughts (Hain et al., 2011) and *(iv)* partitioning of precipitation into runoff and groundwater storage etc. However, accurate estimation of soil moisture is a challenging task given the spatial heterogeneity in terrain, soil composition, interaction with vegetation and aquifers, land management practices, and so forth. The *in-situ* soil moisture measurements are limited, point-based, and show significant spatial variability (Sims and Raman, 2002). Recently, there has been an increase in the use of remotely sensed soil moisture dataset which has been successfully applied to several studies for drought monitoring and severity estimation (Ahmadalipour et al., 2017; Martínez-Fernández et al., 2016; Nicolai-Shaw et al., 2017; Wardlow et al., 2016). However, cloud contamination, low accuracy over dense vegetation cover, and shallow penetration (top few centimeters) remain major drawbacks of the remote sensing approach in understanding the catchment-scale drought dynamics (Srivastava et al., 2016).

Due to the aforementioned factors, the application of simulated soil moisture in drought studies is a viable alternative. Previously, Dai et al. (2004) established a strong correlation between observed soil moisture content (within the top 1 m depth) and Palmer Drought Severity Index (PDSI) during warm-season months for Illinois, Mongolia, China, and Russia. Wang et al. (2011) developed a multi-modal land-surface model approach to study soil moisture drought over China from 1950 through 2006. Otkin et al. (2016) studied the evolution of the extreme flash drought in 2012 using several models, and satellite-derived drought metrics sensitive to soil moisture and vegetation conditions. Sheffield and Wood (2008) provided a global evaluation of drought trends using soil moisture from a hybrid reanalysis–observation forcing dataset. Thober et al. (2015) developed drought forecasting framework using simulated soil moisture based on a combination of the meteorological forecasts from the North American Multi-Model Ensemble (NMME) and the mesoscale hydrologic model (mHM) for Europe. Sehgal et al. (2017) proposed a statistical ensemble of two Land-Surface Models (LSM)-Noah and Mosaic using the *in-situ* soil moisture data for drought analysis for the Contiguous U.S. The study proposed use of the multi-layer soil moisture percentiles in identifying the transient components (onset) of drought from the long-term, severe components (propagation). Li et al. (2016) combined irrigational and reservoir operation in the VIC model to derive soil moisture based drought index for the Tarim River basin, China. Recently, Xu et al. (2018) combined Noah LSM derived soil moisture dataset and retrievals from space-borne Soil Moisture Active Passive (SMAP) soil moisture to develop a standardized soil moisture index for drought monitoring in the Southeastern U.S.

However, most of the studies discussed above employed either large-scale continental (or global) models, or point-scale soil moisture analysis for quantification of drought severity, thus ignoring the intricacies of drought dynamics at a watershed/catchment scale. Accurate soil moisture simulations are essential for reliable drought severity estimations. The variability in soil moisture, accentuated with seasonal variations and influence of hydroclimatology, makes it challenging to estimate droughts using soil moisture accurately. Watershed-scale analysis is crucial to understand the drought dynamics, since the drought generating meteorological conditions propagate from the atmosphere to the hydrological system, and cause a loss of soil moisture, followed by streamflow and groundwater depletion (Mishra and Singh, 2010; Van Loon and Van Lanen, 2012; Van Loon, 2015) Several aspects of drought dynamics like pooling, attenuation, lag, and lengthening manifest at watershed and sub-watershed scales and are significantly influenced by the catchment controls (Eltahir and Yeh, 1999; Peters et al., 2003; Van Lanen et al., 2013). Most large-scale studies miss the variability in the watershed and sub-watershed characteristics that influence the interrelationship between drought and its manifestation in the water balance of the watershed. Recently, Sehgal and Sridhar (2018) used SWAT-simulated water balance components at sub-watershed scale for analyzing the influence of large-scale climatic teleconnections on drought predictability in the SEUS, thus providing impetus to watershed scale drought analysis, in a region like SEUS, with burdened water resources.

This study addresses the existing gap in drought analysis literature by proposing a drought severity assessment approach at watershed-scale by using high-resolution, multi-layer simulated soil moisture from calibrated SWAT models implemented at HUC-12 resolution for 50 watersheds of the Southeastern U.S. The study proposes a multi-scale drought severity assessment using percentiles of stratified soil moisture aggregated to different temporal scales. Furthermore, the study demonstrates the integration of high-resolution SWAT models with the global-scale, short-term meteorological forecasts from CFSv2 for near real-time drought monitoring, and forecasting with a lead of 9-months for 50 watersheds comprising the South-Atlantic Gulf region of Southeastern US. The objectives of this study can be summarized as follows:

a) To implement a stratified drought analysis approach for drought severity estimation. The top soil layer is used for analyzing the transient and low-intensity droughts, and total column soil moisture for long-term, severe droughts, using sub-watershed scale (at HUC-12 resolution) soil moisture dataset obtained by implementing SWAT models for 50 watersheds across the South-Atlantic gulf region of the Southeastern US.
b) To develop a real-time drought monitoring and forecasting framework using high-resolution SWAT based simulated soil moisture, initialized using climate drivers from CFSv2, with a lead-time of up to 9 months, at a weekly time step.
c) To establish the reliability of the proposed approach by comparing the soil moisture based drought severity assessment with a variety of drought indices like PDSI, Palmer Hydrological Drought Index (PHDI), ZNDX and SPI-1, 6, 9 and 12 and observed drought conditions from the USDM.

2. Study area

This study is focused on the South Atlantic-Gulf (SAG) region in the Southeastern US (SEUS) which includes Florida, South Carolina, and Alabama, Georgia, Louisiana, Mississippi, North Carolina, Tennessee, and Virginia in parts (USGS, 2017). The region is listed with a 2-digit Hydrologic Unit Code (HUC) of 03 and consists of 18 sub-regions, each listed with the 4-digit HUC codes ranging from 0301 through 0318. Each HUC-4 basin is further divided into smaller watersheds for this study, totaling 50 for the entire SAG region (Fig. 1), each of which is modeled using SWAT to delineate sub-watersheds matching the HUC-12 resolution as provided by the National Hydrology Dataset plus (NHD +). Table 1 provides the complete list of the 18 basins in the SAG region; each referred to by its HUC− 4 identifier with list and name of the sub-watersheds with the outlet U.S. Geological Survey (USGS) stations. Note that the authors provide the watershed numbers only for easy referencing and identification of these watersheds in the study and should not to be confused with the watersheds at HUC-6 which are larger than these watersheds in most cases. Climatology of the region is provided in Table S1 of the supplimentary material.

Fig. 1. Map showing the location of the study area. The watersheds in the South Atlantic- Gulf (SAG) region are highlighted in grey shade. (For interpretation of the references to colour in this figure legend, the reader is referred to the Web version of this article.)

Table 1
List of the 18 basins in the South Atlantic- Gulf region identified with 4-digit Hydrologic Unit Code with name and a 6-digit identification number (not to be confused with HUC-6) for the constituent watersheds, and, respective outlet USGS stations.

Basin	Watershed	River/basin	Basin	Watershed	River/basin
0301	030101	Roanoke	0309	030902	Caloosahatchee
	030102	Dan	0310	031001	Peace
	030103	Nottoway		031002	Alafia
0302	030201	Tar		031003	Withlacoochee
	030202	Neuse	0311	031101	Suwannee
0303	030301	Lumber		031102	Alapaha
	030302	Black	0312	031201	Ochlockonee
	030303	NE Cape fear	0313	031301	Chattahoochee
0304	030401	Pee Dee		031302	Flint
	030402	Lumber		031303	Apalachicola
	030403	Lynches	0314	031401	Yellow
0305	030501	Catawba		031402	Choctawhatchee
	030502	Congaree		031403	Conecuh
	030503	Edisto	0315	031501	Coosa (Rome)
0306	030601	Savannah		031502	Coosa (Childersburg)
	030602	Barrier Creek		031503	Alabama
	030603	Ogeechee	0316	031601	Noxubee
	030604	Canoochee		031602	Black warrior
0307	030701	Oconee		031603	Tombigbee
	030702	Ocmulgee	0317	031701	Chickasawhay
	030703	Ohoopee		031702	Tallahala
	030704	Satilla		031703	Red Cr.
0308	030801	St. Johns (Geneva)	0318	031801	Pearl (Carthage)
	030802	St. Johns (Buffalo bluff)		031802	Pearl (Monticello)
0309	030901	Arbuckle Cr.		031803	Pearl (Bogalusa)

3. Methodology

3.1. A brief description of the SWAT models

SWAT is a process-based, comprehensive, semi-distributed, continuous-time model (Arnold et al., 2012; Gassman et al., 2007; Neitsch et al., 2011). SWAT is an open-source code simulation model and has been extensively used in hydrological modeling community across the globe with applications in studies ranging from catchment to continental scales (Abbaspour et al., 2015). SWAT simulations incorporate weather, hydrology, sedimentation, soil temperature, plant growth, nutrients, pesticides and land management (Arnold et al., 1998). The model uses weather (precipitation, radiation, and temperature), elevation, soil, land cover/use data to simulate surface and subsurface hydrology and various chemical, biological and sediment fluxes. Hydrologic cycle simulations by SWAT are based on the concept of water balance that closes the budget at the chosen time step.

The ArcSWAT 2010 interface is used to setup and parameterize the model. Sequential Uncertainty Fitting-2 algorithm (Abbaspour et al., 1997, 2004, 2015) is used to calibrate model parameters for each watershed using SWAT-CUP (calibration/uncertainty or sensitivity program) interface for SWAT. A set of 24 parameters are chosen for calibration to address various hydrologic components of the watershed. These parameters include surface runoff (Curve number, soil and plant evaporation, surface runoff and Manning's coefficient, and available soil water capacity, etc.), baseflow (Groundwater “revap”, aquifer – soil interaction, depth of water in the shallow aquifer, time for water leaving the root zone to reach the shallow aquifer, deep aquifer percolation), stormwater (Channel hydraulic conductivity, surface runoff lag time etc.), snow (snowmelt rate, snow temperature) etc. The choice and effect of these parameters are very well documented in SWAT literature (Abbaspour et al., 2015; Arnold et al., 2012; Feyereisen et al., 2007; Jin and Sridhar, 2012; Liu et al., 2008; Uniyal et al., 2015; Van Liew et al., 2005; Wang et al., 2008) and the selected parameters are consistent with the aforementioned studies. For a detailed description of the watershed models, model calibration and validation for the SWAT models used in this study for obtaining various hydrologic variables at HUC-12 resolution, the readers are referred to (Sehgal, 2017).

The basic drivers for SWAT are the U.S. Geological Survey (USGS)-derived Digital Elevation Model (DEM), STATSGO soil layer and land use/cover data from National Land Cover Data (NLCD) 20011 (Homer et al., 2015). One USGS station for each watershed is chosen for calibrating and validating the streamflow generated by the SWAT models. SWAT models are calibrated from1st January 2000 through 31st December 2010 with three years of warm-up period (2000 through 2002) and are validated from 1st January 2011 through 31st December 2013 using the weather data (Precipitation and temperature) from the National Centers for Environmental Prediction (NCEP) Climate Forecast System Reanalysis (CFSR) product (Dile and Srinivasan, 2014; Kang and Sridhar, 2018). The performance assessment of SWAT models is carried out by comparing the SWAT-simulated discharge at the selected outlet with the observed discharge data from the USGS stations using three statistical performance indices, namely, Coefficient of determination (R^2), Normalized Root mean square error (NRMSE) and Willmott's Index (WI) (Willmott et al., 2012, 2015). Watershed-scale performance evaluation of the SWAT models and description of the statistical performance indices is provided in the supplementary material of the paper.

3.2. Integrating SWAT models with CFSv2 data

CFSR has been extended as an operational, real-time product into the future which provides estimates of the atmospheric variables with a lead time of nine months and is initialized at multiple times a day, and, different days of a month (Table 2). Fig. 2 provides a schematic of data assimilation for the study. The precipitation and temperature time series is obtained from CFSv2 data from 1st April 2011 through 19th Dec 2017 by using the first output of CFSv2 models from 1st April 2011 through 12th March 2017, and 9-month forecast data is then obtained from the latest initialization (12th March 2017 in this study). The red ellipse highlights the model run for each initialization which is used for SWAT model implementation with a total number of K initializations from 1st April through 12th Match 2017. The calibrated SWAT models are integrated with CFSv2 drivers from April 2011–December 2017 with a warm-up period of 3 years thus providing simulation outputs from Jan- 2014–December 2017. Combining the retrospective model simulations from SWAT-CFSR integrated models, and the CFSv2 integrated SWAT models, seamless daily simulation outputs are obtained from January 1982–December 2017. A schematic of the entire model setup is provided in Fig. 3.

Table 2
CFSv2 monthly ensembles with respective initial day of the month for four members initialized at 00Z, 06Z, 12Z, and 18Z. (McEvoy et al., 2015).

Initialization Month	Total Members	Initialization Days
January	28	1, 6, 11, 16, 21, 26, 31
February	20	5, 10, 15, 20, 25
March	24	2, 7, 12, 17, 22, 27
April	24	1, 6, 11, 16, 21, 26
May	28	1, 6, 11, 16, 21, 26, 31
June	24	5, 10, 15, 20, 25, 30
July	24	5, 10, 15, 20, 25, 30
August	24	4, 9, 14, 19, 24, 29
September	24	3, 8, 13, 18, 23, 28
October	24	3, 8, 13, 18, 23, 28
November	24	2, 7, 12, 17, 22, 27
December	24	2, 7, 12, 17, 22, 27

3.3. Capturing variability in soil moisture using the appropriate distribution function

Fine-scale heterogeneity in the soil moisture is often parameterized using the variance of the soil moisture data and assuming a particular type of probability density function (PDF) (Famiglietti et al., 2008). In previous studies, normal (Kim et al., 2015), lognormal (Li and Avissar, 1994; Sivapalan and Wood, 1986), gamma (Entekhabi and Eagleson, 1989; Famiglietti and Wood, 1994), extreme value (Brabson et al., 2005) distributions, among others, have been effectively used to estimate the variability in soil moisture data.

A discretized approach is employed in this study to select the suitable distribution function for capturing the soil moisture variability in drought assessment, with the flexibility to account for the seasonal and sub-seasonal, geographic and inter-layer variability at a sub-watershed scale as shown in Fig. 4. This study uses a selection of four distribution functions namely, normal, gamma, lognormal and extreme value to capture soil moisture variability for each layer for each calendar week. Daily soil moisture data is obtained for each sub-watershed (at HUC-12 resolution) for a period of January 1982–December 2013 and averaged over each calendar week. The distribution function with the lowest log-likelihood for weekly soil moisture is chosen for (*i*) fitting the distribution of the soil moisture data from the respective week, (*ii*) calculations of the cumulative distribution function and, (*iii*) percentile estimation for that week of the watershed. A comparison of log-likelihood values for the four distribution functions of soil moisture data for each calendar week, averaged over entire watershed for Roanoke, Satilla, Coosa, and Pearl watersheds is provided in Fig. S2 of the supplementary material. It can be observed that the best choice distribution function changes from week-to-week and watershed-to-watershed, which is effectively accounted in the proposed discretized approach of selection of distribution function for estimating weekly soil moisture percentiles.

3.4. Severity classification of the soil moisture percentile

This study uses soil moisture from two soil layers, namely surface layer (typically extending up to a few centimeters from the ground surface) and the total rooting depth (can extend up to around 2.5 m). Soil moisture from these two profiles has very distinct behavior regarding the persistence and hence their relative response to drought (Sehgal et al., 2017). While the soil surface interacts with the wind, solar radiation, and several other transient weather patterns and provides a platform for the soil-atmospheric interaction, deeper strata interact with the groundwater and are pivotal in surface-groundwater interaction. These factors, when combined with significant heterogeneity in the watershed characteristics like soil type, vegetation, and land use, lead to high spatial variability in the soil moisture from the surface and total column soil moisture and thus, the ability of these strata to respond to drought stress.

The estimated drought severity is tested against the drought severity assessment provided by the US drought monitor (USDM, Svoboda et al. (2002)). USDM provides a county-level, weekly drought assessment of current drought conditions for the US, and is often used as a reference for various socio-economic and agricultural needs, and a popular benchmark for validation other research products for drought monitoring (Hao et al., 2016; He et al., 2015; Wang et al., 2009; Xia et al., 2014).

Here we follow the stratified approach of drought severity assessment from multiple soil layers as proposed by Sehgal et al. (2017) where drought severity estimation using the surface and the total column soil moisture is classified differently. In this study, the drought classification is carried out for the surface, and total column soil profile using the classification provided in Table 3 and drought severity classification from the two layers is compared. While surface soil moisture is used only to capture transient drought conditions, severe and long-term droughts are captured using soil moisture percentiles from total column soil moisture. The top surface percentiles are used to identify droughts in the D0-D3 category only, while, total column soil moisture is used to identify D0 to D4 (all classes) droughts. The highest value among the two layers is then selected as the drought severity for the sub-watershed. For example, assume that the moisture percentile for both layers of a sub-watershed is observed between 5th and 2nd percentile, then the drought severity is classified to be D4 (Extreme drought), however, if top surface soil moisture percentile is less than

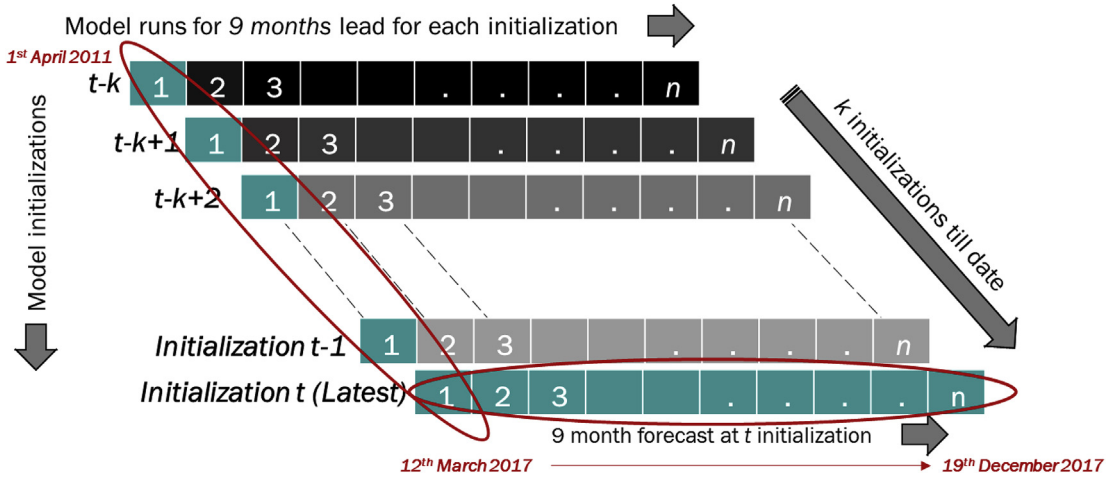

Fig. 2. Data assimilation scheme for precipitation and temperature from the CFSv2 dataset.

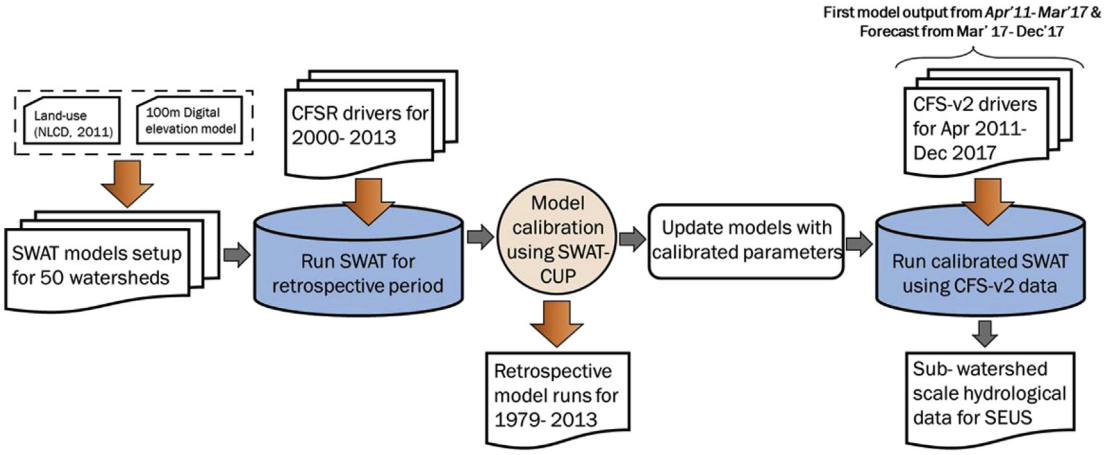

Fig. 3. Schematic of the conceptual framework of forecasting hydrologic variables using the CFSv2 dataset in conjunction with SWAT models for the South-Atlantic Gulf region.

30th percentile while total column soil moisture percentile is still above the 30th percentile, then the drought severity is assessed to be D1 (Abnormally dry).

3.5. Temporal aggregation of the soil moisture percentiles

Suitable aggregation (cumulative value over the period) of soil moisture is important to characterize drought on a range of timescales. Several drought indices, such as SPI, are defined at various time scales to capture long and short-term anomalies. Since the persistence of the surface and the total column soil moisture differ significantly, suitable aggregation of soil moisture from the two layers will be of importance to capture various forms of droughts (transient or long-term; meteorological or hydrological, etc.) in the proposed stratified approach. Shorter temporal aggregation of soil moisture data preserves transient changes in soil moisture while longer aggregation of data smoothens out the percentiles and represent only long-term variations in the data. This study evaluated aggregation of soil moisture to a range of time scales (4-, 8-, 12- 16- and 20 weeks) to select the best aggregation for characterizing drought using a combination of surface and total column soil moisture. Three recent droughts are considered in evaluating the suitability of various aggregations in capturing both transient and long-term drought characteristics effectively at a sub-watershed scale. Chronology of the selected droughts includes 2000–2002, 2006–2009 and 2011–2012.

Fig. 5 provides soil moisture percentiles for Pearl River for the three selected drought periods. For the most part of the three drought periods, the soil moisture percentile for surface and the total column soil moisture can be observed to be less than 30%, as shown in Fig. 5. The effect of different aggregations is evident where higher aggregations (12 and 20 weeks) possess higher persistence and often respond to long-term conditions in soil moisture change with a longer lag. Also, the different response of top surface and total column soil moisture to short-term moisture conditions is evident. For example, from December 2001 through July 2011, surface soil moisture percentiles show three distinct peaks with moisture falling low in the months of February 2011 and May 2011. However, corresponding percentiles from total column soil moisture do not reflect these transient changes. For this study, aggregation of 4 weeks for the top surface soil moisture and 8 weeks for

Table 3
Classification of drought based on layer-wise soil moisture percentiles proposed in this study.

Layer-wise classification of drought severity				
Soil Moisture Percentile	Interpretation	USDM classification	Top layer	Total column
Normal	Normal	D0	D0	D0
Less than 30	Abnormally dry	D1	D1	D1
Less than 20	Moderate Drought	D2	D1	D2
Less than 10	Severe Drought	D3	D2	D3
Less than 5	Extreme Drought	D4	D2	D4
Less than 2	Exceptional Drought	D5	D3	D5

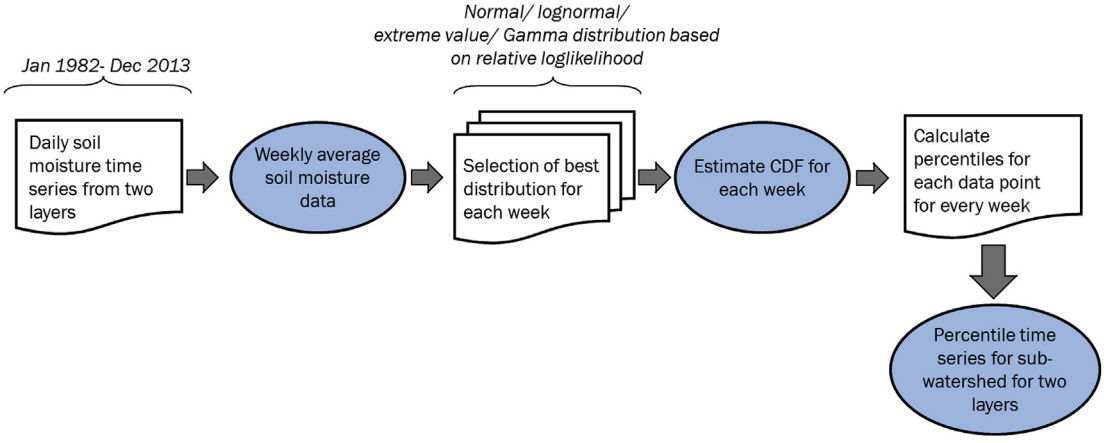

Fig. 4. Schematic for soil moisture percentile calculation at sub-watershed scale.

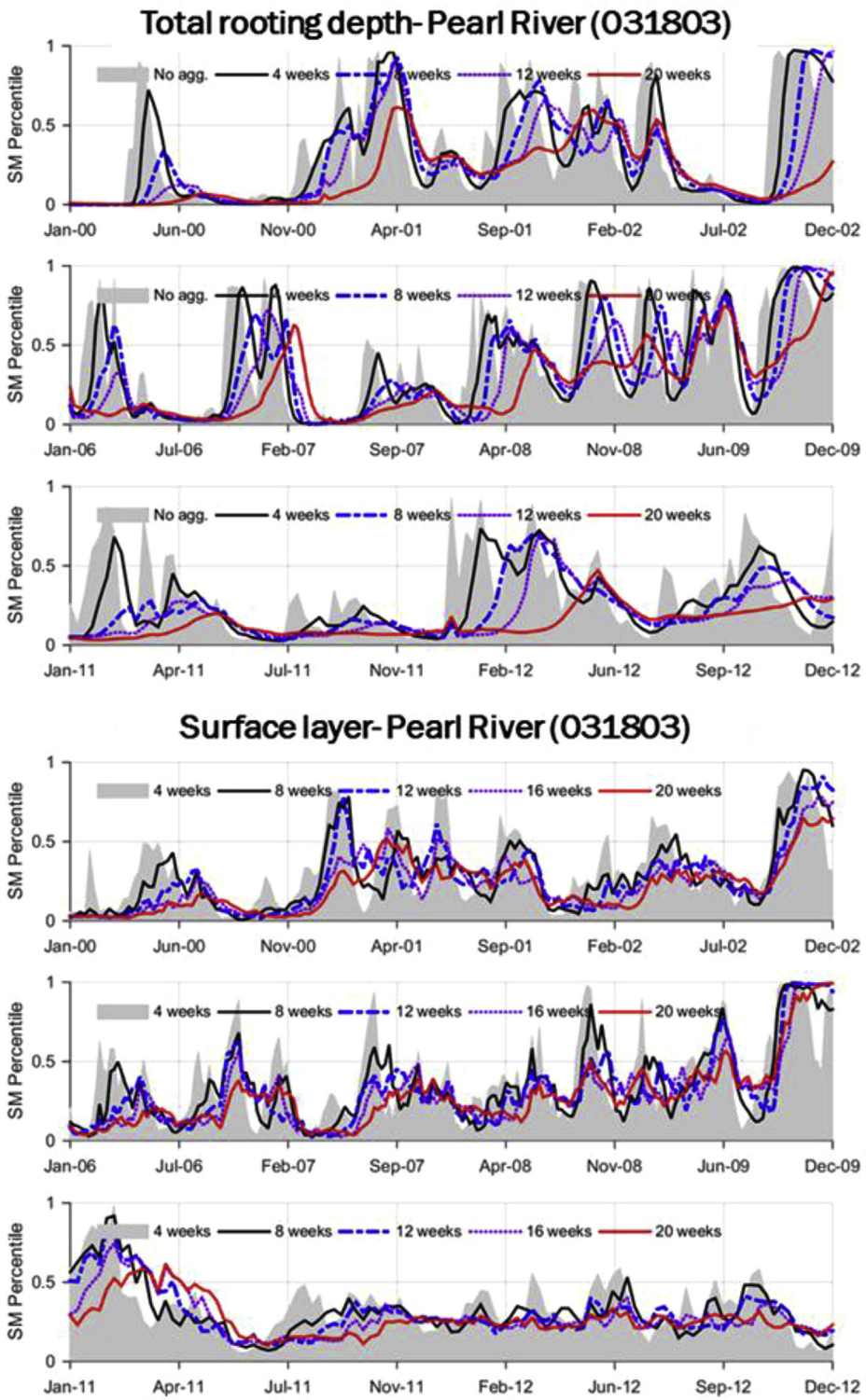

Fig. 5. Comparison of percentiles of the total rooting depth and the surface soil moisture with 4-, 8-, 12-, 16- and 24- weeks aggregation for the three selected drought periods for Pearl watershed.

total column soil moisture is found to be appropriate prior to calculation of soil moisture percentiles to preserve both short and long-term drought signals.

3.6. Accuracy assessment of the estimated drought severity

For performance evaluation, the soil moisture percentiles for the total column and the surface soil moisture with multiple aggregations are compared with several other drought indices provided by National Climatic Data Center (NCDC) repository for 53 climatic divisions in the SAG region. PDSI, PHDI, ZNDX, and SPI for 1, 6, 9, and 12 months are chosen for the comparison with the estimated soil moisture percentiles. The weekly soil moisture values are averaged for the respective month for the sub-watersheds within a climatic division, and a time series of the soil moisture percentile is obtained at a monthly time step for comparison with the NCDC drought indices of the respective climatic

division. Three performance matrices are used in this study to quantify the agreement between PDSI and total column soil moisture percentile (8-weeks aggregated) at the watershed scale for different multiple severity conditions. The matrices are:

a) Index of agreement (IOA):

Number of months soil moisture percentiles correctly captured drought severity per total months the watershed experienced a drought of a given severity.

b) Drought prediction failure (DPF):

Number of months soil moisture percentiles failed to capture drought severity per total month the watershed experienced a drought of a given severity.

c) False alarm (FA):

The number of months soil moisture percentiles reported drought in the absence of actual drought per the total number of months evaluated.

Note that IOA and DPF are complementary to each other and add up to 100%. FA is calculated based on 384-month climatology (January 1982–December 2013). An illustration of DPF, IOA, and FA is provided in Fig. 6. It can be observed that low PDSI values are not reciprocated in retrospective soil moisture percentiles for the 1992–1993 period (DPF). While the year 1998 and 2005 are classified as drought-hit by the proposed approach, the drought conditions are not corroborated by PDSI and SPI-1 (FA). On the other hand, the proposed approach, PDSI, and SPI-1 are in tandem over severe drought in 2000, 2007 and 2013 (Agreement).

4. Results

4.1. Performance evaluation of the reconstructed drought severity

4.1.1. Comparison with PDSI, PHDI, palmer Z index and SPI-1, 6, 9 and 12

Fig. 7 provides a comparison between PDSI, PHDI, Palmer Z index, SPI-1, SPI-6, SPI-9 and SPI-12 with monthly percentiles of the area averaged total column and surface soil moisture aggregated at 4-, 8-, 24-, 36-, 52- weeks, and without any aggregation for the SAG region expressed as correlation coefficient. It can be observed from Fig. 7 that the total column soil moisture percentile has a higher correlation with long-term drought indices (PDSI, PHDI, SPI-6, SPI− 9 and SPI-12) while surface soil moisture percentiles have a higher correlation with palmer Z-index and SPI-1 when no aggregation is used. Increase in aggregation leads to small increase in the correlation between the total column soil moisture with PDSI, PHDI, SPI-6,9 and 12 while the correlation decreases with Z index and SPI-1 with increasing aggregation of total column soil moisture. However, for surface soil moisture, increasing aggregation leads to increase in correlation of soil moisture percentiles with the long-term drought indices, with the highest correlations beyond 24-weeks of aggregation. Due to the shorter response time of Z-index and SPI-1, increasing aggregation has an adverse effect on the correlation with Z-index, and SPI-1 of soil moisture percentiles of both layers. A comparison of the values of PHDI, SPI-6, and Z index and SPI-1 with the total column and surface soil moisture percentiles for a period between January 2000 and December 2013 is provided in Fig. 8. It can be observed from Fig. 8 that the soil moisture percentiles obtained from the SWAT models are able to capture the drought in the study region.

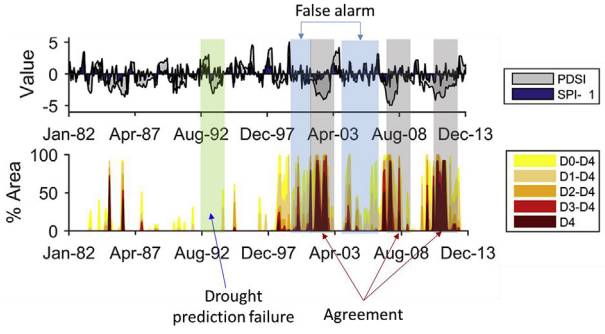

Fig. 6. Illustration of the Index of agreement (IOA), Drought Prediction Failure (DPF) and False Alarm (FA) for a selected watershed. The values of PDSI and SPI-1 are compared with 8-week aggregated total column soil moisture percentiles for January 1982–December 2013.

Fig. 9 shows the IOA, DPF, FA assessment for four drought severities, namely mild (PDSI < 1 and soil moisture percentile < 0.3), moderate (PDSI < 2 and soil moisture percentile < 0.2), severe (PDSI < 3 and soil moisture percentile < 0.1) and exceptional (PDSI < 4 and soil moisture percentile < 0.05). Categorization of these indices based on drought severity classes helps in understanding the relative accuracy of soil moisture percentiles in capturing PDSI of a given severity range. For example, IOA for mild drought gives the agreement values between PDSI and soil moisture percentile when both PDSI and the soil moisture percentile classified drought severity under the mild category for the respective month. It can be seen from Fig. 9 that IOA between PDSI and total column soil moisture percentiles (aggregated to 8-weeks) varies among watersheds and severity classification. Overall, IOA is seen to be above 50% for majority watersheds for mild and moderate droughts. However, IOA is high for the watersheds in Mississippi and Alabama states. While for some of the watersheds especially in the tip of Florida peninsula (watersheds 20–30) the IOA is seen to fall low. This is because of differences in the accuracy of SWAT models for the respective watersheds. Watersheds with a relatively low accuracy while calibrating the SWAT model are expected to show higher disagreement (DPF) with PDSI for the respective watershed. Also, IOA values are lower for most watersheds compared to respective values for lower severity values. This can be attributed to the observation that for most watersheds, low soil moisture percentiles predate PDSI values with similar drought severity, which is more noticeable in higher severity values. Overall, FA is less than 15% of total climatology (384 months) for all watersheds across drought severity values.

4.1.2. Comparison with USDM drought maps

The reconstructed drought maps are compared with the respective USDM drought severity maps to ascertain the accuracy of the proposed drought assessment approach. Fig. 10 provides a comparison of the reconstructed and USDM drought severity maps for two drought periods, February–August 2007, and, May–November 2011. It can be observed from Fig. 10 that the reconstructed drought maps generally predate drought compared to its USDM counterpart, especially during the onset of drought. However, the proposed approach also retains drought persistence longer than the USDM maps owing to the influence of the total column soil moisture with long aggregation (8-weeks). The reconstructed drought maps corresponded well with the area experiencing drought stress. However, overestimation of drought stress can be seen in some of the regions especially in the northeast part of the study area.

4.2. Drought assessment and forecasting using SWAT-CFSv2 integrated model outputs

After having established the accuracy of the proposed stratified approach for retrospective drought analysis using SWAT generated sub-watershed scale (HUC-12 resolution) soil moisture dataset, the approach is expanded to forecast drought severity for 9-months lead time using SWT-CFSv2 integrated hybrid models. SWAT-CFSv2 hybrid

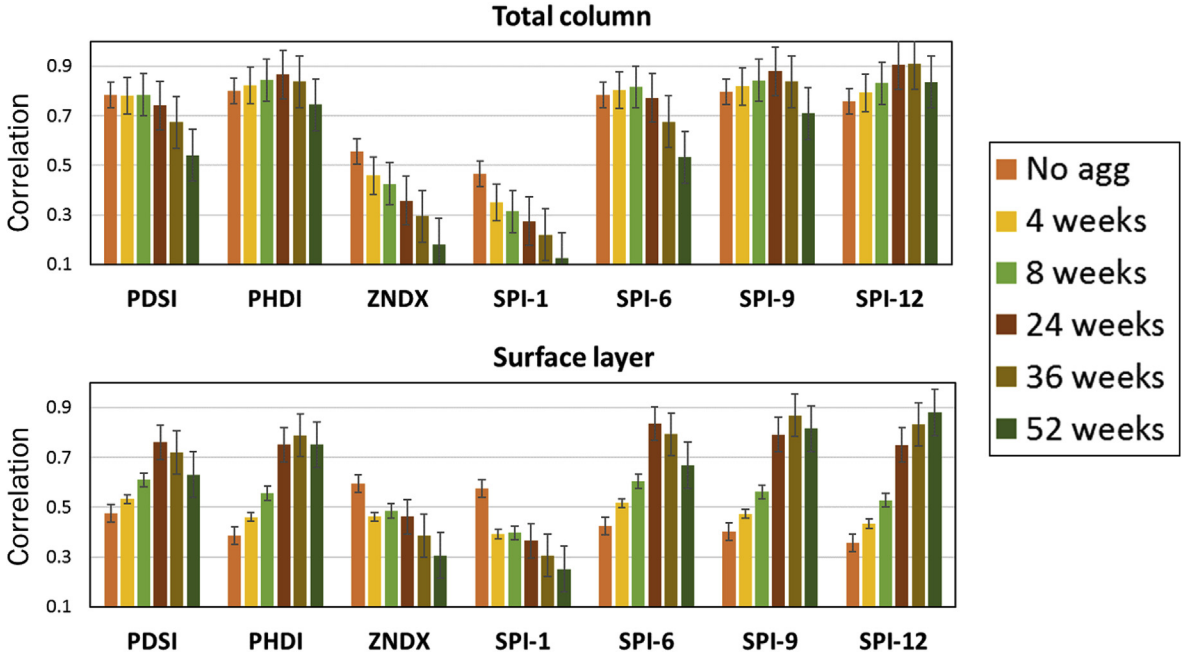

Fig. 7. Comparison between area-averaged reconstructed drought severity and PDSI, PHDI, Palmer Z index, SPI-1, SPI-6, SPI-9 and SPI-12 at different aggregations for 2000–2013, expressed as correlation for the SAG region.

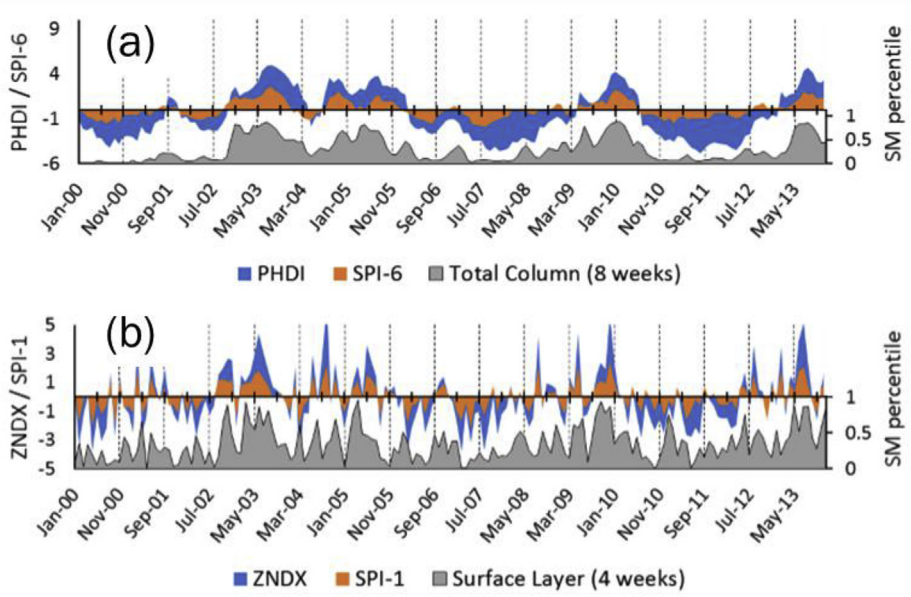

Fig. 8. Comparison of (a) 8-weeks aggregated total column soil moisture percentile with PHDI and SPI-6 (b) 4-weeks aggregated surface soil moisture percentile with Palmer Z-index and SPI-1 between 2000 through 2013.

models provide hydrologic variables from January 2014 through March 2017 in near real-time while the forecasted values are available for 9-months lead, through the third week of December 2017. Soil moisture percentiles are calculated as described in previous sections.

Fig. 11 provides the time series of precipitation (P), change in soil storage ($\Delta S/\Delta T$), Potential Evapotranspiration (PET) and Actual Evapotranspiration (ET) for January 2014–December 2017 using SWAT-CFSv2 integrated models. It can be seen from Fig. 11 that the SWAT-CFSv2 integrated models are able to capture a recent drought in the region in 2016. The period of June–October 2016 is seen to have low soil moisture and precipitation while above normal PET and ET. Time series of weekly soil moisture percentiles from the top and total column soil moisture from SWAT-CFSv2 integrated models is provided in Fig. 12 for the Jan 2014–Dec 2017 period. Fig. 13 provides IOA, FA and DM values between PDSI and total column soil moisture from the SWAT-CFSv2 integrated model (aggregated to 8-weeks) for the January 2014–March 2017 period. Results indicate that high IOA exists between the PDSI and estimated drought severity. For majority watersheds (26 of 45 watersheds in mild category, 34 of 38 in moderate, 18 of 14 in severe and all 7 watersheds in exceptional drought categories respectively), IOA is found to be greater than 60%. Some of the watersheds did not experience any drought in a particular severity class in the period of evaluation and hence no IOA or DM values are assigned to such watersheds (For example 1–10 watersheds in severe drought category). The IOA values increase with increasing severity class indicating that the simulated soil moisture percentiles are very effective

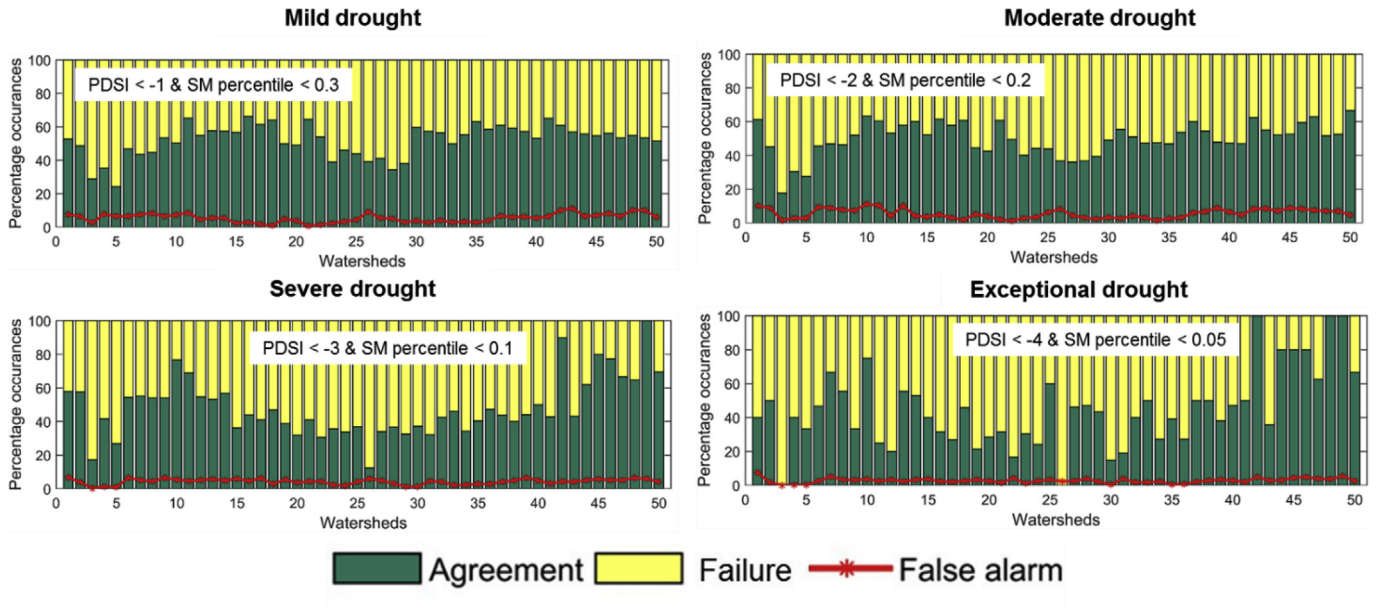

Fig. 9. For all 50 watersheds: Index of Agreement (IOA), Drought prediction failure (DPF) and False Alarm (FA) between PDSI and total column soil moisture (aggregated to 8 weeks) for four drought categories namely mild, moderate, severe and exceptional based on January 1982 through December 2013 climatology.

in capturing severe and extreme drought in near real-time mode using SWAT-CFSv2 model outputs. However, a higher number of FA is observed especially for the mild and moderate drought categories due to higher sensitivity of soil moisture percentiles to transient droughts for these watersheds.

Fig. 14 shows USDM drought maps and the maps generated using SWAT-CFSv2 modeled soil moisture percentiles both computed at a weekly scale, between March 21st and July 6th, 2017. The USDM and simulated drought severity maps have a reasonable degree of spatial association for 1st month (21st March- 18th April). However, the disagreement between the USDM and simulated drought increases with increasing lead time of the forecast. Conditions similar to June–October 2016 are forecasted to occur in mid-2017 leading to drought conditions in the region. Fig. 15 shows the drought severity map for the SAG region showing forecasted drought conditions from April–December 2017. While precipitation of the range of 100 mm in most part of the region is expected to provide relief from drought conditions, moisture deficit during late July and August is forecasted to contribute to building up of dry conditions in Alabama, Georgia, most parts of Florida and parts of Louisiana.

5. Discussion

5.1. Need for a watershed-scale, multi-layer approach for soil moisture based drought assessment

A layer-wise approach is necessary for capturing the dynamics of the surface and subsurface fluxes in the soil column due to the difference in the response time of deeper and surface soil profiles to changing meteorological conditions leading to drought. Moisture availability in the

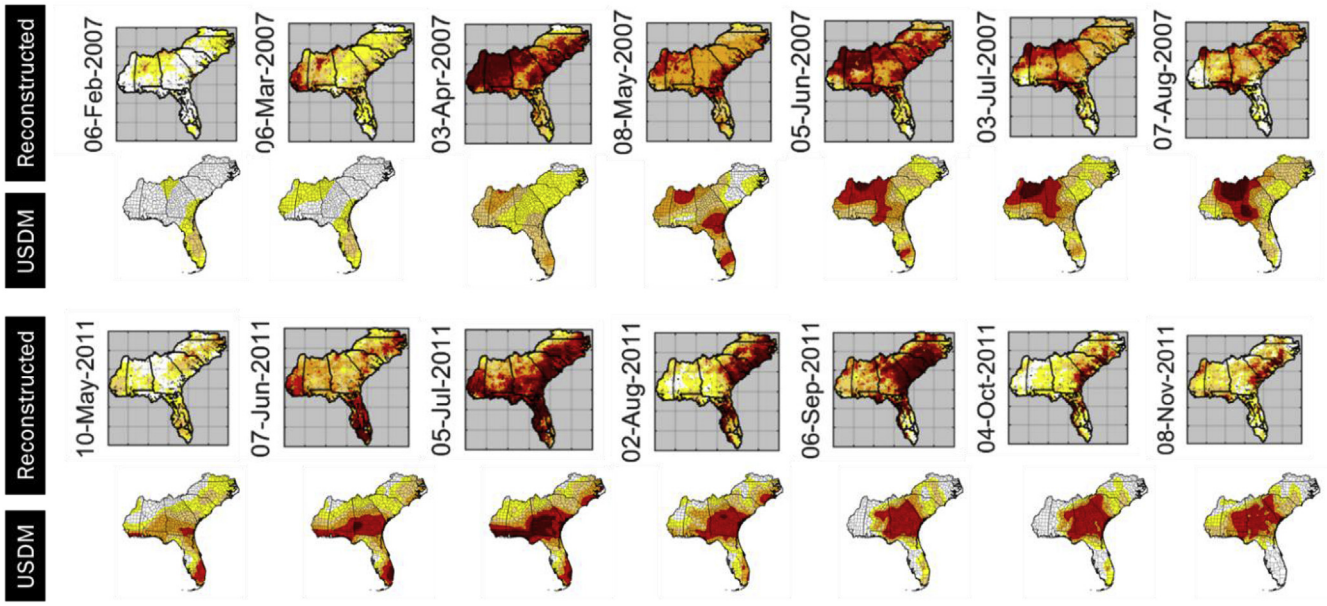

Fig. 10. Weekly drought severity maps for SAG region using the proposed stratified approach compared with the USDM maps, calculated for each first week of the month in February–August 2007 and May–November 2011.

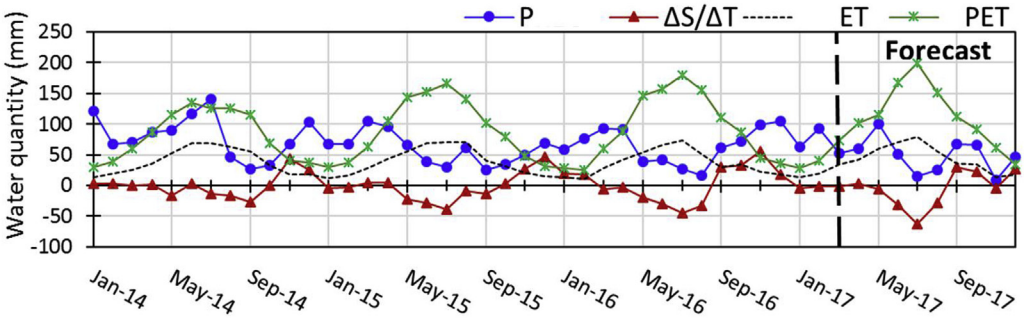

Fig. 11. Area-averaged values of mean monthly precipitation (P), actual evaporation (ET), potential evapotranspiration (PET) and change in soil water storage ($\Delta S/\Delta T$) for the study region using SWAT- CFSv2 integrated models. The dotted black (vertical) line demarcates the SWAT-CFSv2 model warm-up (January 2014 through 12th March 2017) from model forecast period (March through December 2017).

rooting zone indicate water availability for plant uptake, aquifer recharge, and baseflow; and displays variability corresponding to longer time scales, ranging from sub-monthly to seasonal scales. However, the near-surface soil moisture responds to rapid changes in atmosphere related to evaporation and precipitation, thus captures the flash drought scenarios indicating the susceptibility of the watershed to other natural hazards like wildfire (D'Odorico et al., 2000; Sehgal et al., 2017) often at sub-weekly to monthly time scales.

5.2. Seasonal dynamics of soil moisture

Translation of drought-inducing meteorological factors into various hydrological components of the watershed scale water-budget depends on the interaction between several governing factors like vegetative and canopy growth, soil composition, interaction with groundwater, freezing, and thawing of soil, evapotranspiration, etc. While some of these factors (ET, freeze/thaw cycles, etc.) concern only the soil surface, other interactions take place in deeper soil columns thus linking the meteorological fluctuations to soil storage and groundwater. The interplay of the mean and variance of the soil moisture time series for different part of a year is important in selecting the right distribution function to capture soil moisture variability effectively. Furthermore, the variability in soil moisture can be affected by scale (spatial and temporal), season and hydroclimatology of the study region, and can significantly alter the choice of the distributions to estimate the variability in the data. Seasonal and geographical variations in soil moisture variability can be attributed to a combination of factors like hydroclimatology (precipitation, evapotranspiration, transpiration), surface characteristics (soil texture, topography, vegetation, land use and land surface properties, drainage etc.) and infiltration-runoff processes of the study region (Famiglietti et al., 2008; Kim and Barros, 2002; Oldak et al., 2002; Peters-Lidard and Pan, 2002; Teuling and Troch, 2005).

An analysis is carried out in this study to analyze the relationship between the mean and variance of soil moisture for each calendar week for the 50 watersheds which in turn, reflects on the choice of the distribution function to estimate soil moisture variability at the watershed scale. The mean and variance for each week is calculated using the historical simulation (January 1982–December 2013) and later divided by the maximum value for each watershed in order to obtain a comparable range of values across different watersheds. Two distinct phases of the relationship between the mean and variance of week-wise soil moisture are observed (Fig. 16):

a) *Increase in mean soil moisture with decreasing variance*:

This part of the year is marked by increasing mean soil moisture with subsequent weeks whereas the variance in soil moisture is seen to decrease. Empirical fit to this phase shows that an exponential curve can be used to satisfactorily explain the process where the variance in soil moisture for the week is a factor of mean soil moisture through the following relationship:

$$Variance = a' e^{-b`(Mean)} \quad (1)$$

Where $a`$ and $b`$ are constants.

b) *Decrease in mean soil moisture with increasing variance*:

This is a complementary process to *(a)* where the mean soil moisture decreases whereas the variance in soil moisture increases over the weeks. Empirical fir to the data reveals that the interrelationship between variance and mean of soil moisture follows a second-order polynomial function as follows:

$$Variance = aMean^2 + bMean + c \quad (2)$$

Where *a, b* and *c* are constants for the respective sub-watershed.

5.3. Limitations of the study and future work

The proposed methodology of drought analysis and forecasting is comparable to USDM in its representation of drought categories for easy understanding and interpretation of drought conditions by policymakers and water planners. However, the proposed approach and the USDM are different in terms of the data, climatology and interpretation of the respective drought categories. USDM drought maps generally involve many other factors like county-level information on

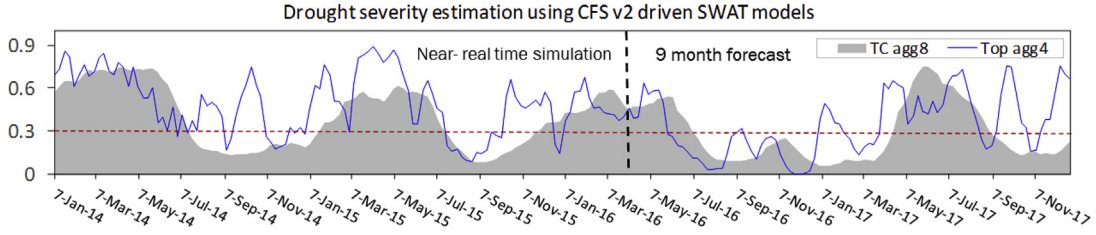

Fig. 12. Weekly percentiles of the area averaged soil moisture for SAG region using 8-weeks aggregated total column soil moisture (shaded in gray), and 4-weeks aggregated surface soil moisture.

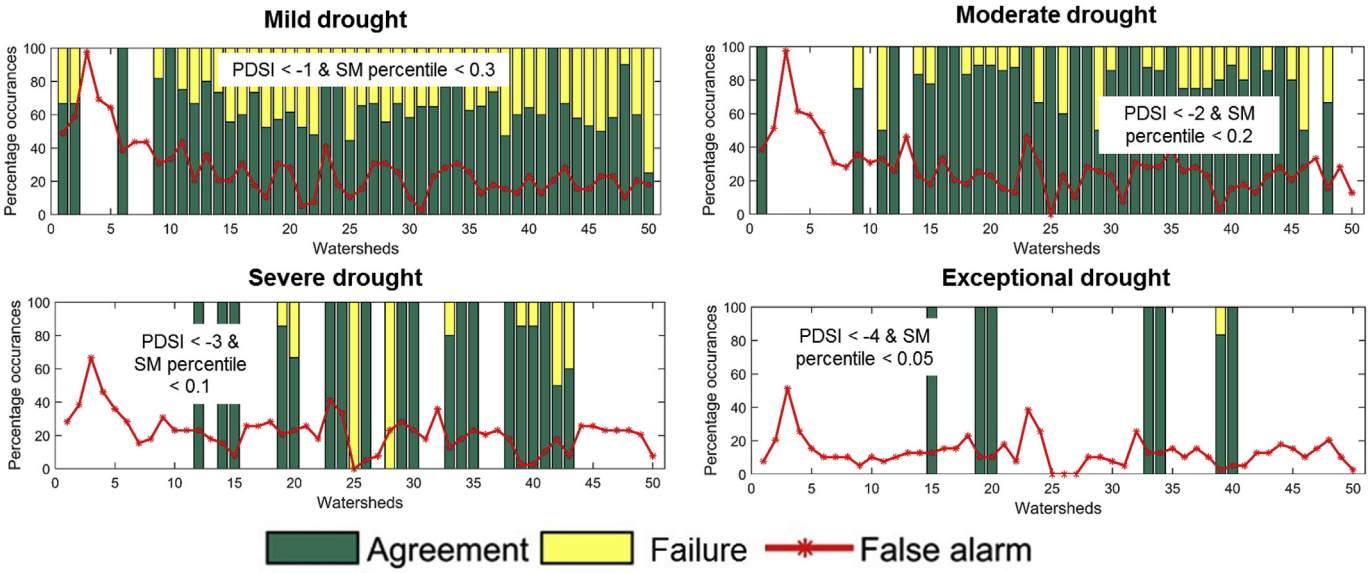

Fig. 13. Same as Fig. 10, but using SWAT-CFSv2 integrated model outputs in near real-time mode for January 2014–March 2017 period.

drought, reservoir levels, snowpack and groundwater (Sehgal et al., 2017; Svoboda et al., 2002) which may lead to different interpretation of drought at local scales. Hence, the hydrological manifestations of the drought representation from the proposed approach may be different from that represented by USDM. In this study, the water deficit, and thus the drought conditions, are estimated by calculating the deviation of the natural conditions of soil moisture from the historical normal values for the respective month or week. However, these extremes may be exasperated by several anthropologic interventions. The difference in the hydrologic/soil moisture/meteorological extremes and the people's perception of drought can be linked to the availability of water for several applications like public water demand, agricultural practices, industrial utilities, recreation, etc. Hence, similar meteorological conditions in one watershed may trigger a different perception of drought in that region compared to another watershed with different geographic conditions, public water needs and/or agricultural applications, etc.

Watershed-scale drought prediction skill is strongly influenced by the SWAT model calibration and the accuracy of the climate drivers. A satisfactory calibration of SWAT models for each watershed ensures model accuracy and the ability to capture the hydrologic variability of the watershed. While the SWAT models perform satisfactorily for the inland watersheds, the calibration performance of the models is relatively weak in the coastal wetlands, especially for the Florida peninsula due to strong tidal influence on the streamflow gaging station used for the model calibration. Extensive basin management and regulated streamflow also influence the performance of the SWAT models negatively, thus limiting the drought predictive skill of the simulated hydrologic variables. However, the performance of the SWAT model is better for larger watersheds due to reduced intermittency and sustained flow regimes. It is worth noting that since all watersheds in the study area (total 50) are independently calibrated and parameterized, the sensitivity of the simulated hydrologic variables to drought generating meteorological conditions may be different, which should be accounted for by the user while implementing the model outputs for drought assessment. The forecasted meteorological drivers from CFSv2 also entail significant uncertainty, which depreciates the drought forecasting

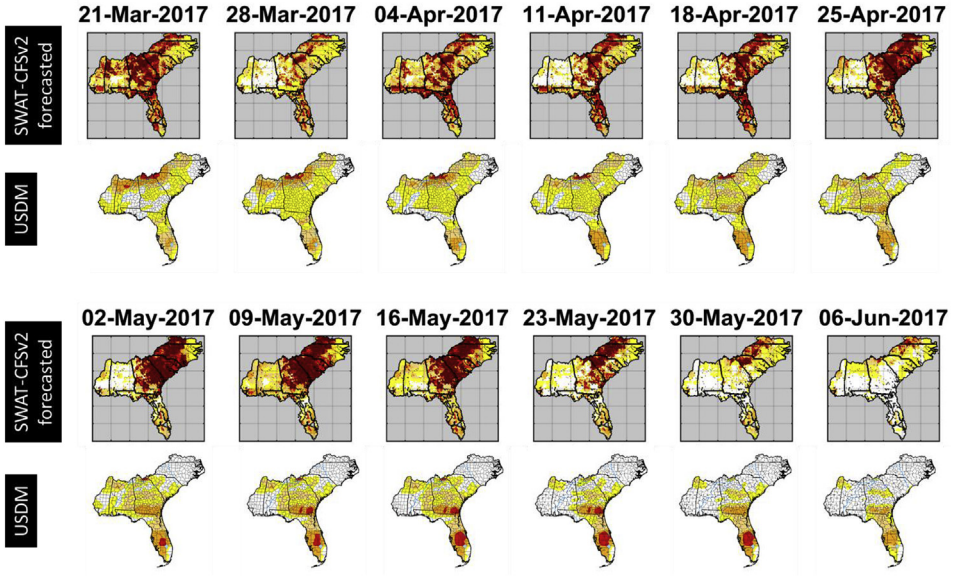

Fig. 14. Comparison of the USDM and simulated drought severity maps using SWAT-CFSv2 integrated models in the forecast mode from 21st March 2017 through 6th June 2017.

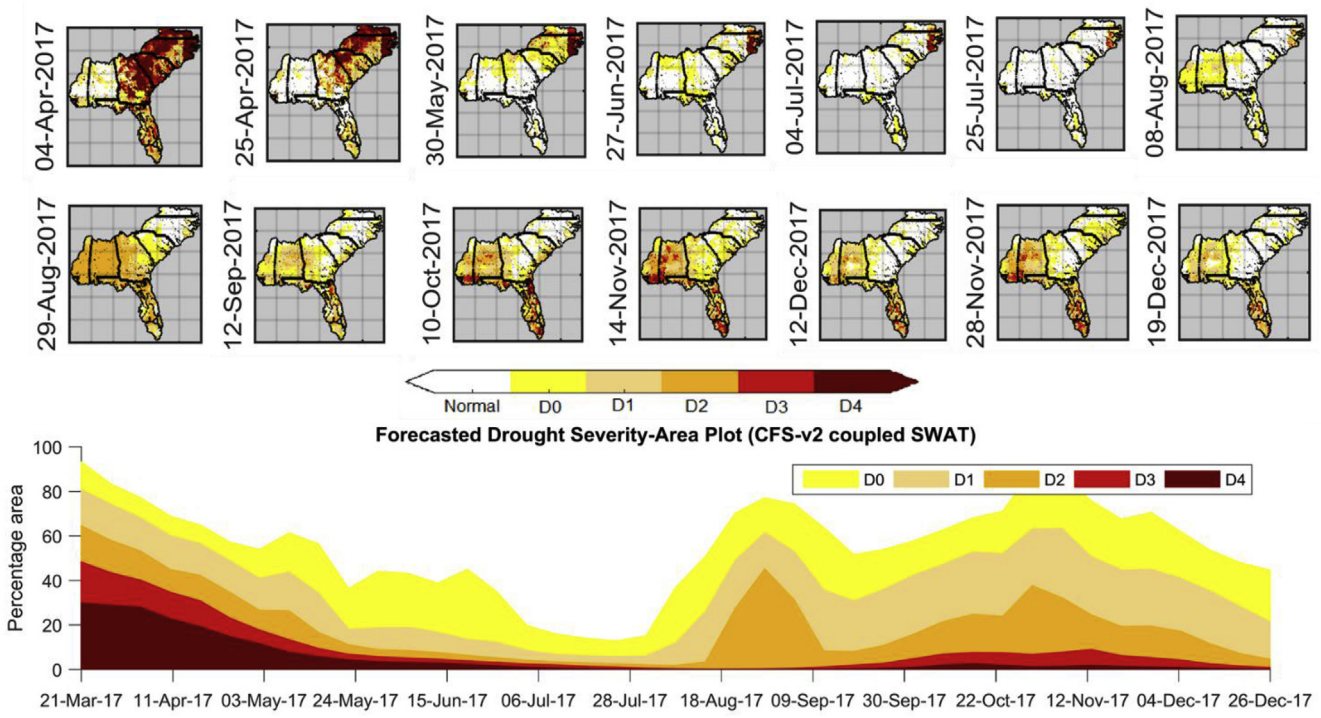

Fig. 15. (Top) Drought severity maps for the South-Atlantic Gulf region using the stratified soil moisture percentile approach using SWAT-CFSv2 integrated soil moisture percentiles for top and total column soil profiles (Bottom) Drought severity-area plot for the forecast period (Third week of March through third week of December 2017 using SWAT-CFSv2 integrated model soil moisture percentiles.

ability of the proposed framework, especially for longer lead-time (> 1 month). While the near real-time drought estimates by the models are reasonably accurate and useful for decision in the study area, the drought forecasts for multi-month lead requires further uncertainty assessment prior to implementation. This study is a proof-of-the-concept for a near real-time, stratified soil moisture based drought monitoring and forecasting framework, by combining a watershed-scale hydrologic model with global-scale climate drivers for regional analysis. Hence, a detailed investigation of the aforementioned limitations remains a topic of future studies.

High-resolution watershed-scale models are helpful in understanding the local-scale hydrologic variability and complex interactions of various bio-physical components. While the application of a multi-layer soil moisture based drought assessment is demonstrated in this study to capture the hydrologic response of watersheds to drought, other hydrologic variables simulated by the models like evapotranspiration, streamflow etc. can as well be used to enhance the scope of application of this study and provide a wholistic view of the response of watersheds under drought. This would be an obvious advantage focussing of a single hydrologic variable and can provide a multi-dimensional (in application and scope) assessment of drought at local scales.

6. Conclusion

This study provides a retrospective drought analysis and a near real-time drought forecasting framework using simulated hydrological variables by SWAT- CFSv2 integrated models for the South-Atlantic Gulf region of the Southeastern US. Retrospective analysis is carried out for a period of 1982 through March 2017, and drought forecasts are provided for a period of March through December 2017 at a weekly time step. The study uses a stratified approach to capture drought onset and persistence using surface soil moisture to characterize low-intensity droughts and total rooting depth soil moisture to capture persistence and severity of severe droughts. The accuracy of the proposed approach is established by comparing the simulated drought maps with those of US drought monitor and other drought indicators provided by NCDC (PDSI, PHDI, Palmer Z index and SPI-1, 6, 9, and 12) for the region. The study finds that the soil moisture percentiles for total rooting depth and surface soil moisture with various aggregations are in good agreement with other long and short-term drought indices provided by NCDC. The important findings of this study are:

a) A stratified approach of using multi-layer soil moisture percentiles for drought severity assessment is helpful in capturing different characteristics of drought. While the surface soil moisture responds to transient drought conditions and captures the onset and spatial propagation of drought, the total rooting depth soil moisture captures the persistence (or sustenance) and vertical propagation (across soil profile) of severe droughts. A combination approach of multi-layer drought assessment provides flexibility (and subjectivity) in better the capturing the space, time and severity aspects of drought.
b) Selection of the suitable temporal aggregation in the development of a multi-layer soil moisture based drought assessment has an important role in determining the sensitivity of the soil moisture percentile to long- or to short-term drought conditions. With longer temporal aggregation (8–24 weeks), the surface soil moisture shows high (> 0.7) correlation with long term drought indices like PDSI and PHDI, similar to the total column soil moisture. This understanding can be of application to the remotely sensed soil moisture as well, where satellite-retrievals are limited to only top few centimeters and is a topic of future research. While there may be some other factors influencing the response of soil profiles to drought, like, soil composition and texture, topography and vegetation etc., which are beyond the scope of this study.
c) Near real-time drought estimation using the SWAT-CFSv2 models, provide promising results for application to the study region, and shows high agreement with PDSI across the study region for all drought categories. Spatial agreement between the USDM and

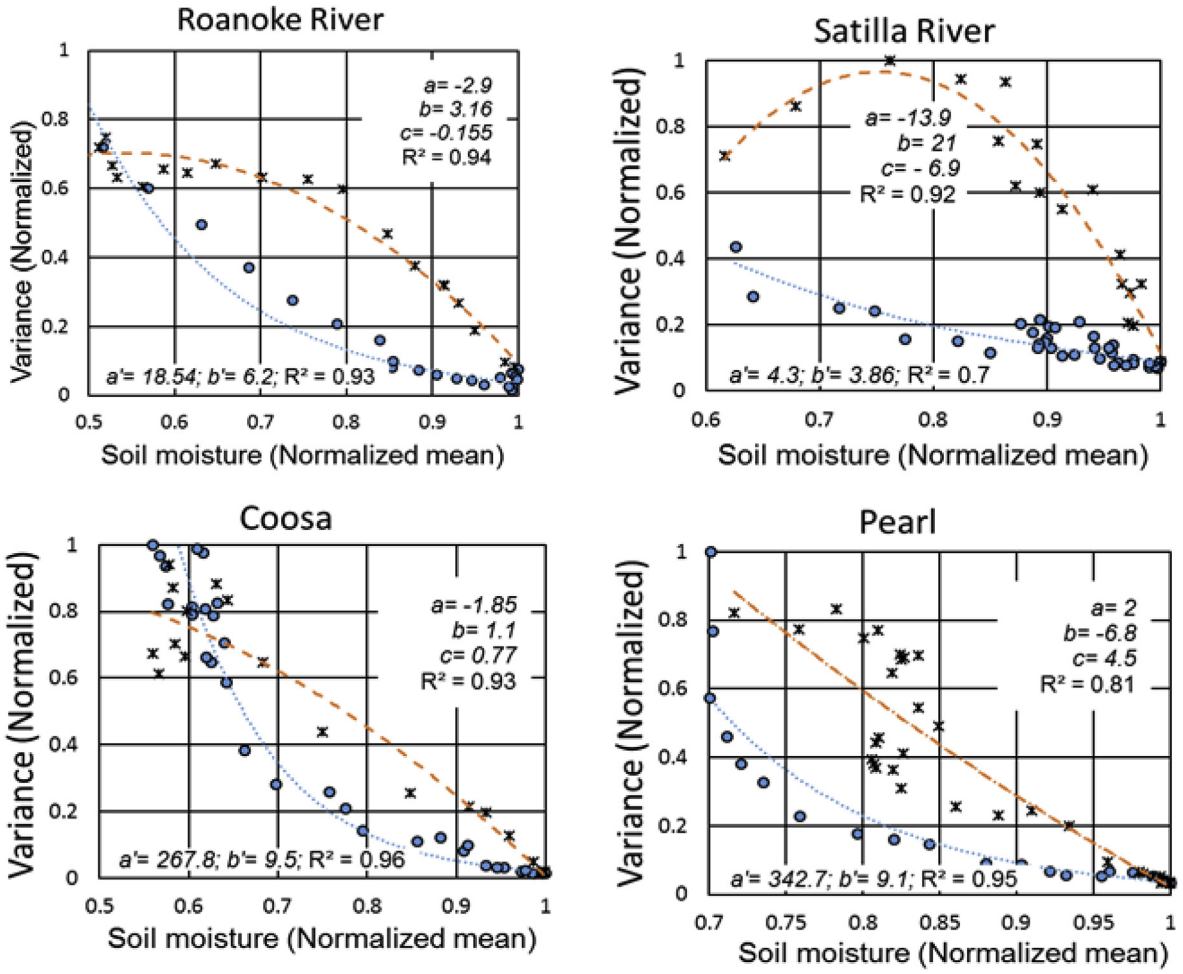

Fig. 16. Relationship between mean and variance of soil moisture for each calendar week for Roanoke, Satilla, Coosa and Pearl River watersheds. The coefficients and R^2 of empirical fit to the watershed scale mean and variance of soil moisture for all calendar weeks of a year is provided.

proposed approach has some obvious discrepancies in classification of the drought into same severity classes. This can be attributed to *(i)* the formulations of the drought estimation approach using both surface and total column soil profile, which leads to higher sensitivity to developing drought conditions *(ii)* Calibration accuracy of the SWAT models for the respective watersheds, which vary due to several factors including suitable parameterization and calibration of the model, watershed characteristics, etc.

d) The drought forecasting ability of the SWAT-CFSv2 models require attention, as there is large disagreement between observed drought maps from the USDM and the estimated drought severity, especially with lead-time over 1-month. These brings into light the uncertainty associated with the global-scale weather forecasts for the study region, especially for a long lead-time.

Acknowledgement

This project was funded, in part, by the Virginia Agricultural Experiment Station (Blacksburg) and the Hatch Program of the National Institute of Food and Agriculture, U.S. Department of Agriculture (Washington, D.C.). We are grateful that the Advanced Research Computing facility at Virginia Tech was made available for our simulation analysis. We are also thankful for the financial support from Virginia Tech's Open Access Subvention Fund.

Appendix A. Supplementary data

Supplementary data to this article can be found online at https://doi.org/10.1016/j.wace.2018.100191.

References

Abbaspour, K., Genuchten, M.v., Schulin, R., Schläppi, E., 1997. A sequential uncertainty domain inverse procedure for estimating subsurface flow and transport parameters. Water Resour. Res. 33 (8), 1879–1892.

Abbaspour, K., Johnson, C., Van Genuchten, M.T., 2004. Estimating uncertain flow and transport parameters using a sequential uncertainty fitting procedure. Vadose Zone J. 3 (4), 1340–1352.

Abbaspour, K., et al., 2015. A continental-scale hydrology and water quality model for Europe: calibration and uncertainty of a high-resolution large-scale SWAT model. J. Hydrol. 524, 733–752.

Ahmadalipour, A., Moradkhani, H., Yan, H., Zarekarizi, M., 2017. Remote Sensing of Drought: Vegetation, Soil Moisture, and Data Assimilation, Remote Sensing of Hydrological Extremes. Springer, pp. 121–149.

Arnold, J.G., et al., 2012. SWAT: model use, calibration, and validation. Transact. ASABE 55 (4), 1491–1508.

Arnold, J.G., Srinivasan, R., Muttiah, R.S., Williams, J.R., 1998. Large Area Hydrologic Modeling and Assessment Part I: Model Development1. Wiley Online Library.

Brabson, B., Lister, D., Jones, P., Palutikof, J., 2005. Soil moisture and predicted spells of extreme temperatures in Britain. J. Geophys. Res.: Atmosphere 110 (D5).

D'Odorico, P., Ridolfi, L., Porporato, A., Rodriguez-Iturbe, I., 2000. Preferential states of seasonal soil moisture: the impact of climate fluctuations. Water Resour. Res. 36 (8), 2209–2219.

Dai, A., Trenberth, K.E., Qian, T., 2004. A global dataset of Palmer Drought Severity Index for 1870–2002: relationship with soil moisture and effects of surface warming. J. Hydrometeorol. 5 (6), 1117–1130.

Dile, Y.T., Srinivasan, R., 2014. Evaluation of CFSR climate data for hydrologic prediction in data-scarce watersheds: an application in the Blue Nile River Basin. JAWRA J. Am.

Water Resour. Assoc. 50 (5), 1226–1241.
Eltahir, E.A., Yeh, P.J.F., 1999. On the asymmetric response of aquifer water level to floods and droughts in Illinois. Water Resour. Res. 35 (4), 1199–1217.
Entekhabi, D., Eagleson, P.S., 1989. Land surface hydrology parameterization for atmospheric general circulation models including subgrid scale spatial variability. J. Clim. 2 (8), 816–831.
Famiglietti, J., Wood, E., 1994. Multiscale modeling of spatially variable water and energy balance processes. Water Resour. Res. 30 (11), 3061–3078.
Famiglietti, J.S., Ryu, D., Berg, A.A., Rodell, M., Jackson, T.J., 2008. Field observations of soil moisture variability across scales. Water Resour. Res. 44 (1).
Feyereisen, G., Strickland, T., Bosch, D., Sullivan, D., 2007. Evaluation of SWAT manual calibration and input parameter sensitivity in the Little River watershed. Trans. ASABE (Am. Soc. Agric. Biol. Eng.) 50 (3), 843–855.
Gassman, P., Reyes, M., Green, C., Arnold, J., 2007. The Soil and Water Assessment tool: historical development, applications, and future research directions. Trans. ASABE (Am. Soc. Agric. Biol. Eng.) 50 (4), 1211–1250.
Hain, C.R., Crow, W.T., Mecikalski, J.R., Anderson, M.C., Holmes, T., 2011. An intercomparison of available soil moisture estimates from thermal infrared and passive microwave remote sensing and land surface modeling. J. Geophys. Res.: Atmosphere 116 (D15).
Hansen, J.W., 2005. Integrating seasonal climate prediction and agricultural models for insights into agricultural practice. Philos. Trans. R. Soc. Lond. B Biol. Sci. 360 (1463), 2037–2047.
Hao, Z., et al., 2016. A statistical method for categorical drought prediction based on NLDAS-2. J. Appl. Meteorol. Climatol. 55 (4), 1049–1061.
He, B., Liao, Z., Quan, X., Li, X., Hu, J., 2015. A global grassland drought index (GDI) product: algorithm and validation. Rem. Sens. 7 (10), 12704–12736.
Homer, C.G., et al., 2015. Completion of the 2011 National Land Cover Database for the conterminous United States-Representing a decade of land cover change information. Photogramm. Eng. Rem. Sens. 81 (5), 345–354.
Jin, X., Sridhar, V., 2012. Impacts of Climate Change on Hydrology and Water Resources in the Boise and Spokane River Basins1. Wiley Online Library.
Kang, H., Sridhar, V., 2017. Combined statistical and spatially distributed hydrological model for evaluating future drought indices in Virginia. J. Hydrol. Region. Stud. 12, 253–272. https://doi.org/10.1016/j.ejrh.2017.06.003.
Kang, H.W., Sridhar, V., 2018. Improved drought prediction using near real-time climate forecasts and simulated hydrologic conditions. Sustainability 10, 1799. https://doi.org/10.3390/su10061799.
Kim, G., Barros, A.P., 2002. Space–time characterization of soil moisture from passive microwave remotely sensed imagery and ancillary data. Rem. Sens. Environ. 81 (2), 393–403.
Kim, J., Mohanty, B.P., Shin, Y., 2015. Effective soil moisture estimate and its uncertainty using multimodel simulation based on Bayesian Model Averaging. J. Geophys. Res.: Atmosphere 120 (16), 8023–8042.
Li, B., Avissar, R., 1994. The impact of spatial variability of land-surface characteristics on land-surface heat fluxes. J. Clim. 7 (4), 527–537.
Li, Z., et al., 2016. An agricultural drought index to incorporate the irrigation process and reservoir operations: a case study in the Tarim River Basin. Global Planet. Change 143, 10–20.
Liu, Y., Yang, W., Wang, X., 2008. Development of a SWAT extension module to simulate riparian wetland hydrologic processes at a watershed scale. Hydrol. Process. 22 (16), 2901–2915.
Manuel, J., 2008. Drought in the Southeast: lessons for water management. Environ. Health Perspect. 116 (4), 168–171.
Martínez-Fernández, J., González-Zamora, A., Sánchez, N., Gumuzzio, A., Herrero-Jiménez, C., 2016. Satellite soil moisture for agricultural drought monitoring: assessment of the SMOS derived Soil Water Deficit Index. Rem. Sens. Environ. 177, 277–286.
McEvoy, D.J., Huntington, J.L., Mejia, J.F., Hobbins, M.T., 2015. Improved seasonal drought forecasts using reference evapotranspiration anomalies. Geophys. Res. Lett. 43, 377–385. https://doi.org/10.1002/2015GL067009.
Mishra, A.K., Singh, V.P., 2010. A review of drought concepts. J. Hydrol. 391 (1), 202–216.
Nagy, R., Lockaby, B.G., Helms, B., Kalin, L., Stoeckel, D., 2011. Water resources and land use and cover in a humid region: the southeastern United States. J. Environ. Qual. 40 (3), 867–878.
Neitsch, S.L., Arnold, J.G., Kiniry, J.R., Williams, J.R., 2011. Soil and Water Assessment Tool Theoretical Documentation Version 2009. Texas Water Resources Institute.
Nicolai-Shaw, N., Zscheischler, J., Hirschi, M., Gudmundson, L., Seneviratne, S.I., 2017. A drought event composite analysis using satellite remote-sensing based soil moisture. Rem. Sens. Environ. 203, 216–225.
Oldak, A., Jackson, T.J., Pachepsky, Y., 2002. Using GIS in passive microwave soil moisture mapping and geostatistical analysis. Int. J. Geogr. Inf. Sci. 16 (7), 681–698.
Otkin, J.A., et al., 2016. Assessing the evolution of soil moisture and vegetation conditions during the 2012 United States flash drought. Agric. For. Meteorol. 218, 230–242.
Pederson, N., et al., 2012. A long-term perspective on a modern drought in the American Southeast. Environ. Res. Lett. 7 (1) 014034.
Peters-Lidard, C., Pan, F., 2002. Re-thinking the Contradictions of Soil Moisture Spatial Variability. AGU Fall Meeting Abstracts, pp. 1042.
Peters, E., Torfs, P., Van Lanen, H., Bier, G., 2003. Propagation of drought through groundwater—a new approach using linear reservoir theory. Hydrol. Process. 17 (15), 3023–3040.
Scasta, J.D., Weir, J.R., Stambaugh, M.C., 2016. Droughts and wildfires in western US Rangelands. Rangelands 38 (4), 197–203.
Seager, R., Tzanova, A., Nakamura, J., 2009. Drought in the southeastern United States: causes, variability over the last millennium, and the potential for future hydroclimate change. J. Clim. 22 (19), 5021–5045.
Sehgal, V., 2017. Near real-time seasonal drought forecasting and retrospective drought analysis using simulated multi-layer soil moisture from hydrological models at sub-watershed scales. Virginia Tech. http://hdl.handle.net/10919/78623.
Sehgal, V., Sridhar, V., 2018. Effect of hydroclimatological teleconnections on the watershed-scale drought predictability in the Southeastern US. Int. J. Climatol. https://doi.org/10.1002/joc.5439.
Sehgal, V., Sridhar, V., Tyagi, A., 2017. Stratified drought analysis using a stochastic ensemble of simulated and in-situ soil moisture observations. J. Hydrol. 545, 226–250.
Shafiee-Jood, M., Cai, X., Chen, L., Liang, X.Z., Kumar, P., 2014. Assessing the value of seasonal climate forecast information through an end-to-end forecasting framework: application to US 2012 drought in central Illinois. Water Resour. Res. 50 (8), 6592–6609.
Sheffield, J., Wood, E.F., 2008. Global trends and variability in soil moisture and drought characteristics, 1950–2000, from observation-driven simulations of the terrestrial hydrologic cycle. J. Clim. 21 (3), 432–458.
Sims, A.P., Raman, S., 2002. Adopting drought indices for estimating soil moisture: a North Carolina case study. Geophys. Res. Lett. 29 (8).
Sivapalan, M., Wood, E., 1986. Spatial Heterogeneity and Scale in the Infiltration Response of Catchments, Scale Problems in Hydrology. Springer, pp. 81–106.
Srivastava, P.K., Petropoulos, G., Kerr, Y.H., 2016. Satellite Soil Moisture Retrieval: Techniques and Applications. Elsevier.
Svoboda, M., LeComte, D., Hayes, M., Heim, R., 2002. The drought monitor. Bull. Am. Meteorol. Soc. 83 (8), 1181.
Teuling, A.J., Troch, P.A., 2005. Improved understanding of soil moisture variability dynamics. Geophys. Res. Lett. 32 (5).
Thilakarathne, M., Sridhar, V., 2017. Characterization of future drought conditions in the Lower Mekong Basin. Weather Climate Extrem. 17, 47–58. https://doi.org/10.1016/j.wace.2017.07.004.
Thober, S., et al., 2015. Seasonal soil moisture drought prediction over Europe using the North American Multi-Model Ensemble (NMME). J. Hydrometeorol. 16 (6), 2329–2344.
U.S. Census Bureau, P.D., Washington D.C., 2005. Interim state population pro-jections. U.S. Census Burea.
Uniyal, B., Jha, M.K., Verma, A.K., 2015. Parameter identification and uncertainty analysis for simulating streamflow in a river basin of Eastern India. Hydrol. Process. 29 (17), 3744–3766.
USGS, 2017. Boundary Descriptions and Names of Regions, Subregions, Accounting Units and Cataloging Units.
Van Lanen, H., Wanders, N., Tallaksen, L., Van Loon, A., 2013. Hydrological drought across the world: impact of climate and physical catchment structure. Hydrol. Earth Syst. Sci. 17 (5), 1715–1732.
Van Liew, M.W., Arnold, J., Bosch, D., 2005. Problems and potential of autocalibrating a hydrologic model. Transactions of the ASAE 48 (3), 1025–1040.
Van Loon, A., Van Lanen, H., 2012. A process-based typology of hydrological drought. Hydrol. Earth Syst. Sci. 16 (7), 1915.
Van Loon, A.F., 2015. Hydrological drought explained. Wiley Interdisciplin. Rev.: Water 2 (4), 359–392.
Wang, A., Bohn, T.J., Mahanama, S.P., Koster, R.D., Lettenmaier, D.P., 2009. Multimodel ensemble reconstruction of drought over the continental United States. J. Clim. 22 (10), 2694–2712.
Wang, A., Lettenmaier, D.P., Sheffield, J., 2011. Soil moisture drought in China, 1950–2006. J. Clim. 24 (13), 3257–3271.
Wang, X., Yang, W., Melesse, A.M., 2008. Using hydrologic equivalent wetland concept within SWAT to estimate streamflow in watersheds with numerous wetlands. Trans. ASAE (Am. Soc. Agric. Eng.) 51 (1), 55.
Wardlow, B., et al., 2016. Remote Sensing of Drought: Emergence of a Satellite-based Monitoring Toolkit for the United States, Remote Sensing of Water Resources, Disasters, and Urban Studies. CRC Press, pp. 367–398.
Willmott, C.J., Robeson, S.M., Matsuura, K., 2012. A refined index of model performance. Int. J. Climatol. 32 (13), 2088–2094.
Willmott, C.J., Robeson, S.M., Matsuura, K., Ficklin, D.L., 2015. Assessment of three dimensionless measures of model performance. Environ. Model. Software 73, 167–174.
Xia, Y., et al., 2014. Application of USDM statistics in NLDAS-2: optimal blended NLDAS drought index over the continental United States. J. Geophys. Res.: Atmosphere 119 (6), 2947–2965.
Xu, Y., Wang, L., Ross, K.W., Liu, C., Berry, K., 2018. Standardized soil moisture index for drought monitoring based on soil moisture active passive observations and 36 Years of North American land data assimilation system data: a case study in the Southeast United States. Rem. Sens. 10 (2), 301.
Zou, L., Xia, J., She, D., 2017. Drought characteristic analysis based on an improved PDSI in the wei River basin of China. Water 9 (3), 178.